Available online at www.sciencedirect.com
SCIENCE DIRECT®
Applied Surface Science 236 (2004) 473–478
applied surface science
www.elsevier.com/locate/apsusc

Photoelectron spectroscopy study of oxygen vacancy on vanadium oxides surface

Qi-Hui Wu[a,*], A. Thissen[a], W. Jaegermann[a], Meilin Liu[b]

[a]*Department of Materials Science, Surface Science Institute, Darmstadt University of Technology, Darmstadt 64283, Germany*
[b]*School of Materials Science and Engineering, Georgia Institute of Technology, Atlanta, GA 30332, USA*

Accepted 14 May 2004

Available online 2 July 2004

Abstract

The thermal properties of vanadium pentoxide (V_2O_5) thin films have been studied by X-ray photoelectron spectroscopy (XPS) and ultraviolet photoelectron spectroscopy (UPS). XPS and UPS data demonstrate that V_2O_5 thin films are gradually reduced by annealing in the ultrahigh vacuum chamber at temperatures up to 400 °C due to the formation of oxygen vacancy. The oxygen defect in the remaining thin film leads to the appearance of a new emission line at about 10.3 eV in the valence bands, which is direct evidence for oxygen vacancy on a solid surface.

PACS: 79.60

Keywords: Vanadium pentoxide; XPS; UPS; Oxygen vacancy

1. Introduction

V_2O_5 is a transition metal oxide with interesting potential for technological applications [1]. It has been studied intensively by theoretical calculation and experimental techniques [2,3]. Polycrystalline films exhibit multicoloured electrochromism allowing the use in electrochromic displays, colour filters, and other optical devices [4,5]. In addition, bulk and thin films of V_2O_5 have been used as an oxidation catalyst [6]. As a functional inorganic material, V_2O_5 can be used in gas sensors [7]. All these interesting properties are strongly related to oxygen vacancies leading to changes in the electronic structure and to crystal relations. Thin film V_2O_5 can be prepared by a variety of deposition techniques. The performance of the active layer is strongly dependent on the synthesis procedure [8]. Different techniques, such as sol–gel process [9], dc- and rf-magnetron sputtering [10,11], pulsed laser deposition [12], and plasma enhanced metalorganic chemical vapor deposition (MOCVD) [13] as well have been applied to prepare V_2O_5 thin films. The reduction behaviour and phase transitions of vanadium oxides at various conditions have already been studied [14–17]. But the detailed processes and mechanism is still unclear [14–19]. In this

* Corresponding author. Present address: Materials Science and Engineering, Georgia Institute of Technology, Atlanta, GA 30332-0245, USA. Tel.: +1 4048 9412 47; fax: +1 4048 9491 40.
E-mail address: qihui.wu@mse.gatech.edu (Q.-H. Wu).

0169-4332/$ – see front matter © 2004 Elsevier B.V. All rights reserved.
doi:10.1016/j.apsusc.2004.05.112

communication, the V_2O_5 thin films have been prepared by physical vapour deposition (PVD) with the aim to study their thermal properties. The main techniques in this study are XPS and UPS, which are the common method to investigate the occupied electronic (core- and valence-) states in a solid [17,20,21]. XPS is used to determine the composition of the V_2O_5 surfaces and the oxidation states of the elements. UPS provides the information about the electronic structure of the valence band region.

2. Experimental

V_2O_5 thin films were deposited on freshly cleaved highly orientated pyrolytical graphite (HOPG) substrates at room temperature (RT) from a homemade PVD effusion cell using a BN crucible attached by a NiCr/Ni thermocouple in ultrahigh vacuum (UHV) chamber. During deposition the source temperature was approximately 670 °C at a pressure of about 1.2×10^{-6} mbar indicating the partial reduction of V_2O_5 in the crucible. The XPS and UPS experiments were carried out at room temperature in a multichamber UHV system combining different in situ preparation techniques connected to a transfer chamber with the surface analysis system (Phi 5700). The base pressure during the measurements was better than 10^{-9} mbar. Al Kα radiation ($hv = 1486.6$ eV) from a monochromatized X-ray source is used for XPS. A UV light ($hv_1 = 21.22$ eV (HeI) and $hv_2 = 40.81$ eV (HeII)) from a discharge lamp is for UPS measurements. The spectra are given in binding energy (BE) referred to the Fermi level of a sputter cleaned Ag reference sample. Sample stoichiometry ratios $S_{i,j}$ are calculated from the XP spectra using the following formula [22]:

$$S_{i,j} = \frac{C_i}{C_j} = \frac{I_i/\mathrm{ASF}_i}{I_j/\mathrm{ASF}_j} \quad (1)$$

where C_i and C_j are the concentrations of the elements, I_i and I_j the background corrected intensities of the photoelectron emission lines and ASF_i and ASF_j the atomic sensitivity factors for photoionization of the ith and jth elements. For example the O to V ratio in stoichiometric V_2O_5 should be $S_{O,V} = 2.5$. Formula (1) is only valid for homogenous element distributions in the sample.

3. Results and discussions

The O 1s and V 2p core level XP spectra of step by step deposited V_2O_5 thin films are shown in Fig. 1. The line width of V $2p_{1/2}$ is much broader than that of V $2p_{3/2}$ due to the Coster-Kronig Auger transitions [23]. The binding energies of the V 2p levels are 516.9 and 524.5 eV for V $2p_{3/2}$ and V $2p_{1/2}$, respectively, with a splitting of 7.6 eV, whereas that of the O 1s level is 529.6 eV. These are very close to the literature values for stoichiometric V_2O_5 at room temperature [24]. The V $2p_{3/2}$ peak shows up well shaped even for lowest coverage with a very weak shoulder line on the low binding energy side due to a small amount of V^{4+} species. The binding energies of the V $2p_{3/2}$ and O 1s core levels do not change appreciably with increasing V_2O_5 coverage. The spectra appear similar for all the investigated coverage, and a growing film of the same oxide composition after each growth step is evident. The ratio of $S_{O,V}$ for different deposition steps is calculated according to the formula (1) and shown in Fig. 2. A value of about 2.46 ± 0.04 is found, indicating again that the V_2O_5 thin films are nearly stoichiometric.

Fig. 3 shows the XP spectra of the O 1s and V 2p core level emission lines before (a) and after (b–d) reduction by heating in UHV chamber at the specified temperatures (from 100 °C to 400 °C) for about 1 h. Spectrum (e) is subsequently heated in oxygen with a partial pressure of 10^{-6} mbar at 400 °C after spectrum (d). Spectra (b–d) show that the V $2p_{3/2}$ and V $2p_{1/2}$ lines become broader and shift to lower binding

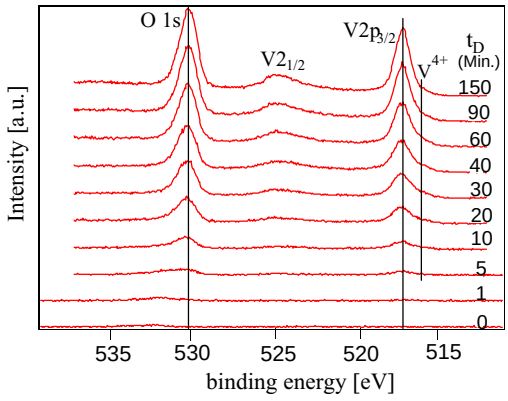

Fig. 1. O 1s and V 2p core level XP spectra of successive deposition of V_2O_5.

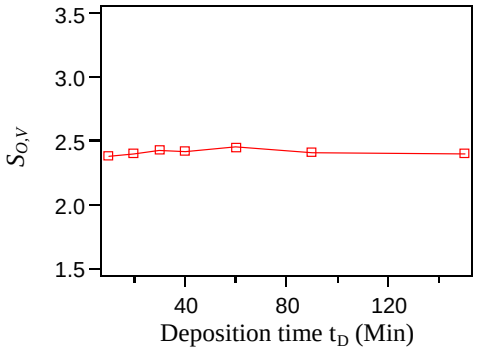

Fig. 2. The ratio of O 1s/V 2p as the function of deposition time.

energies with increasing temperature. The decrease in the binding energy of the core level (chemical shift) usually indicates a decrease in the positive charge of the transition metal atoms. The O 1s line is slightly asymmetric, suffers a small shift to higher binding energies (∼0.3 eV), and becomes a little broader due to the formation of V_2O_{5-x} species [25] with the full width at half maximum (FWHM) increasing from 1.25 to 1.45 eV. In spectrum (e) we note that the V 2p emission lines are slightly shifted back to higher binding energy after heating in oxygen atmosphere indicating a slight re-oxidation of vanadium ions. In order to analyse the reduction process in more detail, the background corrected XP spectra of the V $2p_{3/2}$ lines were fitted by Voigt lines (see Fig. 4). The

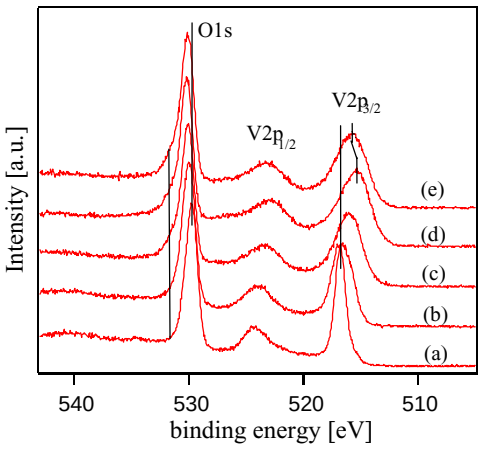

Fig. 3. XP spectra of O 1s and V 2p core level before (a) and after heat treatments in UHV chamber (b) 200 °C, (c) 300 °C, (d) 400 °C, and (e) 400 °C with 10^{-6} mbar oxygen.

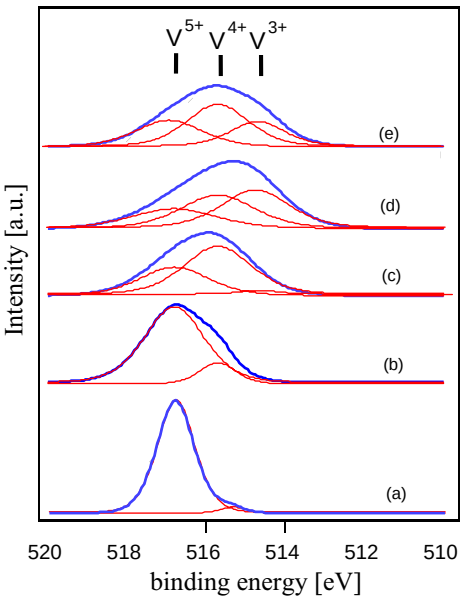

Fig. 4. Fitted data of V $2p_{3/2}$ lines after removal of background for different treatments in UHV chamber: (a) RT, (b) 200 °C, (c) 300 °C, (d) 400 °C, (e) 400 °C in 10^{-6} mbar oxygen.

binding energy difference between V^{5+} and V^{4+} and between V^{4+} and V^{3+} is about 1.0 eV [23]. At 200 °C only V^{4+} species are formed. With increasing temperature, V^{3+} species grows up gradually. When heated in oxygen (spectrum (e)), the intensity of V^{3+} species decreases again and that of V^{4+} species increases compared with spectrum (d) due to some part of V^{3+} ions are re-oxidised to V^{4+} oxidation state again.

The intensity ratios of $S_{O,V}$ calculated with formula (1), the average oxidation states of vanadium (n) calculated from the fitted data as $5 \times V^{5+}\% + 4 \times V^{4+}\% + 3 \times V^{3+}\%$ and the central BEs of the V $2p_{3/2}$ line are presented in Table 1. The decrease of the $S_{O,V}$

Table 1
$S_{O,V}$, n, and binding energies (BEs) of V $2p_{3/2}$

Temperatures (°C)	$S_{O,V}$	n	BEs
RT	2.46	4.96	516.9
200	2.33	4.75	516.6
300	2.00	4.25	516.1
400	1.75	3.86	515.3
400 in O_2	1.90	4.08	515.7

ratios implies the decomposition of V_2O_5 at higher temperatures. The removal of the originally negatively charged oxygen ion as neutral species leads to the reduction of the nearest-neighbour vanadium. The defect electrons will become localised at the vanadium, which will be discussed based on the UPS data later on. This leads to the formation of V^{4+} and even V^{3+} in the vicinity of the vacancy. The removal of oxygen from the V_2O_5 lattice also causes the formation of defect phases in the resulting film [26]. We note that the $S_{O,V}$ ratio shows a small increase and vanadium becomes slightly oxidised after heating in oxygen as shown in spectrum e. It implies that oxygen atoms can re-enter the crystal lattice of V_2O_5. From Table 1, the effective charge transfer per oxygen (ECTO) can be calculated as

$$\mathrm{ECTO} = \frac{n(1) - n(2)}{S_{O,V}(1) - S_{O,V}(2)} \quad (2)$$

where (1) and (2) refer to two consecutive treatments. The ECTOs for different temperatures are shown in Table 2. Therefore an average of 1.5 ECTO is estimated, which is 0.5 electrons higher than Bullett's result [27]. This result implies that with one oxygen atom leaving from the V_2O_5 crystal only about 1.5 extra electrons locate on the vanadium ions, not 2 electrons as expected.

Table 2
The effective charge transfer per oxygen in V_2O_5

RT–200 °C	200–300 °C	300–400 °C	400–400 °C in O_2
1.4	1.5	1.5	1.5

Fig. 5 reports the valence band spectra measured from the same samples as those shown in Fig. 2, (a) is valence band XPS (VB-XPS), (b) is HeI UPS and (c) is HeII UPS. In both XP and UP valence band spectra, it is clear that with increasing temperature, a broad line at ~1.3 eV grows up gradually. The feature at ~1.3 eV can be assigned as V 3d state [28]. It appears due to the charge transfer to V^{5+} ions from the removed oxygen as neutral charge, which leads to an occupation of originally empty V 3d state forming the conduction band, and then form V^{4+} and V^{3+} ions. V_2O_5 is a non-magnetic insulator. The ligand coordination around the V ions in V_2O_5 deviates from the ideal octahedra and direct metal–metal interactions are very weak. The broadening in the V 3d emission is probably given

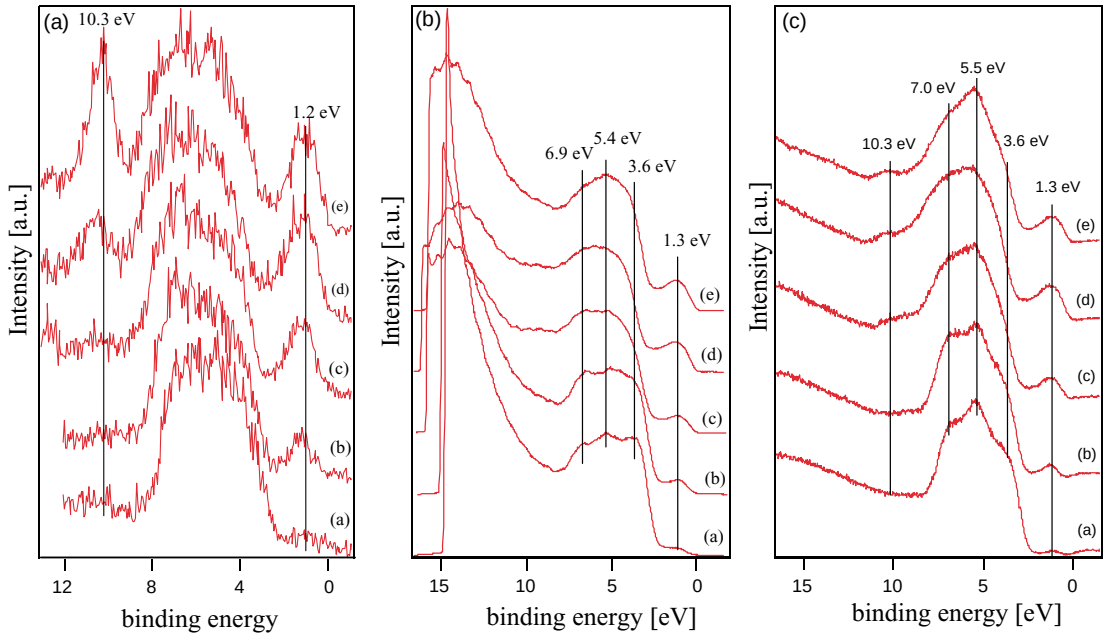

Fig. 5. Valence bands of V_2O_5 thin films measured from the same samples as shown in Fig. 2: (a) XPS, (b) HeI (21.2 eV), and (c) HeII (40.8 eV).

by the variation in boundary distance and geometric bonding of the V sites. At the same time the peak at ~10.3 eV exhibits a similar tendency. In the UP spectra there are three distinct lines between 3 and 8 eV, they exhibit a well defined valence band shape with binding energies at about 3.6, 5.5 and 7.0 eV, respectively. When the heating temperature is increased, the intensities of the emissions at 3.6 and 5.5 eV decrease clearly, whereas that of 7.0 eV peak is nearly constant. These phenomena have already been observed by Heber and Grünert [17]. It is interesting to observe that the emission line at 5.5 eV increases evidently when the sample is heated in oxygen. The shoulder appearing at ~10.3 eV is located near to the position of OH emissions [29]. However, the feature is not observed as prepared sample (spectrum (a)) and presents after thermal evacuation in UHV and is significantly increased with heating temperatures. Moreover, its intensity increases parallel to the V 3d peak. Therefore, it does not likely originate from OH- or H_2O-adsorbates. Heber and Grünert [17] simply assigned it as band bending in the vicinity of V^{4+} defects. The feature at ~10.3 eV is also found on $La_{0.5}Sr_{0.5}FeO_3$ (LSF) surface, which does not contain vanadium ions, after heated at 400 and 600 °C in UHV chamber with oxygen partial pressure of 10^{-6} mbar (see Fig. 6). The intensity of line at ~10.3 eV increases dramatically when the heating temperature increases from 400 to 600 °C. So that the peak at ~10.3 eV is not likely due to the certain percentage of the valence-band signal that is shifted by ~1.3 eV to higher binding energy. LSF is a popular cathode electrode for solid oxide fuel cells [30], the formation of oxygen vacancy is very important for oxygen ions transfer inside the lattices [31]. From above results, the signal is probably due to oxygen defects on the surface [26], which has been discussed above because its intensity increases with decrease of $S_{O,V}$. We note that after heating in oxygen at 400 °C the intensity of the feature at ~10.3 eV in the XP spectrum does not decrease, but increases, which is different from the signal of HeII spectrum. It is probably due to that at higher temperatures the concentration of oxygen defects will continue to dipper surface, which can be probed by VB-XPS but not by UPS [17].

From the HeI spectra (see Fig. 5b), the change of work function has been calculated as hv_1 (21.22)-BE_{SEO} (where BE_{SEO} is the binding energy of secondary emission onset) and shown in Fig. 7. It decreases with increasing temperature and increases again when heated in oxygen. This phenomenon is possibly due to the concentration change of reduced V species on the surface. The higher the concentration of V^{4+} and V^{3+} species the more electrons are transferred to the V ions in the surface leading to a decrease in the work function. From Fig. 7, it is obvious that the work function of the sample after heated at 400 °C in oxygen is slightly higher than that after heated at 300 °C, which means that the concentration of V^{4+} and V^{3+} ions on the sample after heated at 400 °C with oxygen partial pressure of 10^{-6} mbar is lower than the sample after heated at 300 °C in UHV chamber. From this result, the oxidation state of the V ions on the

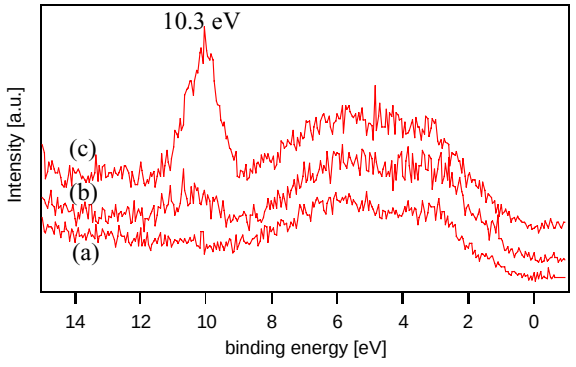

Fig. 6. XPS valence spectra of powder $La_{0.5}S_{0.5}FeO_3$ before (a) and after heat treatments in UHV chamber, (b) 400 °C, and (c) 600 °C.

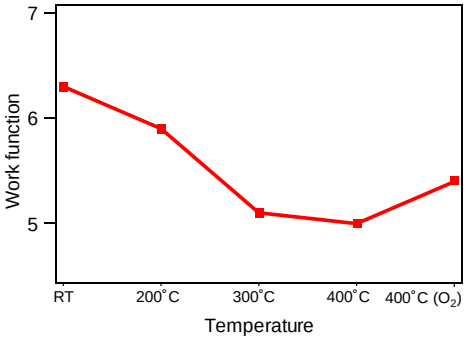

Fig. 7. The changes of work function of thin V_2O_5 film after different treatment steps as calculated from HeI spectra.

sample surface after heated at 400 °C in O_2 should be higher than that after heated treatment at 300 °C. But in the XPS data (see Table 1) a lower oxidation state of vanadium ion is found for the sample heated at 400 °C in O_2 atmosphere. These results are consistent with the comparison of valence band spectra because the escape depth in XPS and UPS is different, as have been mentioned before that UPS is much sensitive technique on the topmost surface [17,32]. These results imply that the re-oxidation reaction only occurs in the topmost surface region but not in the bulk. This is the reason why the intensity of feature at ~10.3 eV increase after heated at 400 °C with oxygen partial pressure of 10^{-6} mbar in VB-XP spectrum. Based on above results and discussions, the feature at ~10.3 eV can be assigned to a crystal defect due to an oxygen vacancy, which can be more easily probed by VB-XPS.

In summary, XPS and UPS measurements show that the V_2O_5 is gradually reduced from V^{5+} to V^{4+} and further to V^{3+} due to the formation of oxygen vacancy, when it is heated in UHV chamber up to 400 °C. The V ions will be partially re-oxidised, when sub-stoichiometric V_2O_5 thin films are heated in O_2 with a partial pressure of 10^{-6} mbar. The oxygen defect in the remaining thin film leads to the appearance of a new emission line at about 10.3 eV in the valence bands, which is useful evidence to detect the oxygen vacancy in the field of high temperature chemistry, for example solid oxide fuel cell.

Acknowledgements

The authors would like to thank the Deutsche Forschungsgemeinschaft (DFG) for financial support.

References

[1] A. Talledo, C.G. Granqvist, J. Appl. Phys. 77 (1995) 4655.
[2] W. Lambrecht, B. Djafari-Rouhani, M. Lannoo, J. Vennik, J. Phys. C: Solid State Phys. 13 (1980) 2485.
[3] E.A. Meulenkamp, W. van Klinken, A.R. Schlatmann, Solid State Ionics 126 (1999) 235.
[4] Y. Fujita, K. Miyazaki, T. Tatsuyama, Jpn. J. Appl. Phys. 24 (1985) 1082.
[5] S.F. Cogan, N.M. Nguyen, S.T. Perrotti, R.D. Rauph, Proc. Soc. Photo-Opt. Instrum. Eng. 57–62 (1988) 1016.
[6] L. Fiermans, P. Clauws, W. Lambrecht, L. Vandeabroucke, J. Vennik, Phys. Status Solidi A 59 (1980) 485.
[7] Y. Shimizu, K. Nagase, N. Miura, N. Yamazoe, Jpn. J. Appl. Phys. 29 (1990) L1708.
[8] C.G. Granquist, Handbook of Inorganic Electrochromic Materials, Elsevier Science, Amsterdam, 1995.
[9] N. Ozer, Thin Solid Films 305 (1997) 80.
[10] J. Cui, D. Da, W. Jiang, Appl. Surf. Sci. 133 (1998) 225.
[11] X.J. Wang, H.D. Li, Y.J. Fei, X. Wang, Y.Y. Xiong, Y.X. Nie, K.A. Feng, Appl. Surf. Sci. 177 (2001) 8.
[12] G.J. Fang, Z.L. Liu, Y. Wang, Y.H. Liu, K.L. Yao, J. Vac. Sci. Technol. A 19 (2001) 887.
[13] H. Watanabe, K.-I. Itoh, O. Matsumoto, Thin Solid Films 386 (2001) 281.
[14] J. Haber, M. Witko, R. Tokarz, Appl. Catal. A Gen. 157 (1997) 3.
[15] R.J.D. Tilley, B.G. Hyde, J. Phys. Chem. Solid 31 (1970) 1613.
[16] D.S. Su, M. Wieske, E. Beckmann, A. Blume, G. Mestl, R. Schlogl, Catal. Lett. 75 (2001) 81.
[17] M. Heber, W. Grünert, J. Phys. Chem. B 104 (2000) 5288.
[18] K. Devriendt, H. Poelman, L. Fiermans, Surf. Sci. 433–435 (1999) 734.
[19] D.S. Su, R. Schloyl, Catal. Lett. 87 (2002) 115.
[20] M. Heber, W. Grünert, Top. Catal. 15 (2001) 3.
[21] A.C. Dupuis, M. Abu Haija, H. Kuhlenbeck, H.J. Freund, Surf. Sci. 539 (2003) 99.
[22] C.D. Wagner, W.M. Riggs, L.E. Davis, J.F. Moulder, Handbook of X-ray Photoelectron Spectroscopy, Perkin Elmer Corporation, Eden prairie, 1979.
[23] E. Antonides, E.C. Janse, G.A. Sawatzky, Phys. Rev. B 15 (1977) 4596.
[24] M. Witko, K. Hermann, R. Tokarz, Catal. Today 50 (1999) 553.
[25] G.A. Sawatzky, D. Post, Phys. Rev. B 20 (1979) 1546.
[26] C.V. Ramana, O.M. Hussain, B. Srinivasulu Naidu, P.J. Reddy, Thin Solid Films 305 (1997) 219.
[27] D.W. Bullett, Solid State Phys. 35 (1980) 129;
D.W. Bullett, J. Phys. C: Solid State Phys. 13 (1980) L595.
[28] R.G. Egdell, M.R. Harrison, M.D. Hill, L. Porte, G. Wall, J. Phys. C: Solid State Phys. 17 (1984) 2889.
[29] J. Connor, M. Considine, H. Hiller, D. Briggs, J. Electron Spectrosc. Relat. Phenom. 12 (1977) 143.
[30] S.P. Simner, J.P. Shelton, M.D. Anderson, J.W. Stevenson, Solid State Ionics 161 (2003) 11.
[31] B.C.H. Steele, J. Power Sourc. 49 (1994) 1.
[32] M. Heber, W. Grünert, Top. Catal. 5 (2001) 3.